# NUMERICAL ANALYSIS OF THE NICHE EFFECT ON THE DIFFUSE SOUND TRANSMISSION LOSS OF PARTITION PANELS

Michiel Lannoye[1], Daniele Giannini[1], Stijn François[1], Edwin P.B. Reynders[1]

[1] *Department of Civil Engineering, KU Leuven, Belgium*





## Abstract

When predicting the sound transmission loss (STL) of a partition panel in indoor (room-wall-room) conditions, the sound fields on both sides are often assumed to be diffuse. The resulting STL is then independent of the detailed room geometries and represents the average panel performance over an ensemble of source and receiver rooms. Using the reciprocity relation between direct field radiation and diffuse reverberant loading, the STL of a panel of arbitrary complexity can be computed by modeling the partition panel deterministically and coupling that model to acoustic halfspace models at both sides. So far, this approach has mainly been applied to flat baffled interfaces, for which the halfspace radiation stiffness can be obtained from the Rayleigh integral. However, extending the framework to more complex radiation geometries has remained challenging. In this work, the direct field radiation stiffness is computed using a coupled finite element-boundary element (FE-BE) approach. As a validation example, the effect of a laboratory niche on the diffuse STL is investigated. The niche air volume is modeled using FE, while radiation into the acoustic halfspace is treated using BE. The approach is validated against experimental STL results of a laminated glazing.

**Keywords:** *building acoustics, niche effect, diffuse sound transmission loss, FE-BE coupling*

## 1. Introduction

For indoor sound insulation predictions, the sound fields in the source and receiver rooms are often assumed to be diffuse [1]. Under this assumption, the predicted sound transmission loss (STL) represents an average response over an ensemble of rooms, rather than the response for one specific room geometry. In this work, the diffuse STL is computed using a hybrid deterministic-statistical energy analysis (Det-SEA) room-wall-room framework, in which the partition panel with arbitrary geometry and boundary conditions is modeled deterministically and the adjacent rooms are described statistically as diffuse fields [1]. The diffuse field reciprocity relationship relates the diffuse reverberant loading on the panel to its direct field radiation into an acoustic halfspace [2]. Consequently, the computation requires a model of the panel and of the direct field radiation on both sides. For flat baffled interfaces, this radiation stiffness can be obtained from the Rayleigh integral [3]. However, this approach is restricted to flat interfaces and cannot directly account for more complex radiation geometries, such as panels mounted in a niche.

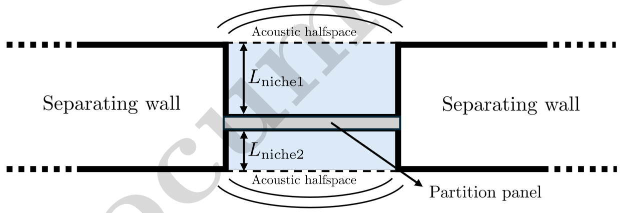


**Figure 1:** Visualization of a partition panel in a niche.

A niche is a form of geometric recess as the depth of the aperture of the wall is larger than the thickness of the considered panel. A practical example in buildings is a window. The mounting of a partition panel in a niche is often observed in laboratory conditions, where the partition panel is placed between two reverberant rooms, as visualized schematically in Fig. 1. The difference in thickness of the testing panel and the separating wall results in a niche.

Experimental studies have shown that the niche geometry can significantly influence the STL determined in a laboratory [4], [5], [6]. The position of the partition panel in the niche plays an important role. A panel placed at the center of the niche resulted in the

***Corresponding author:*** *michiel.lannoye@kuleuven.be.*

lowest STL values, while at one of the edges of the aperture, the highest STL was obtained [4], [7]. These factors mainly cause issues with the reproducibility of experimental measurements, especially for frequencies below the critical frequency of the partition panel [5], [7]. Above the critical frequency, the effect of the position of the plate in the niche is less prominent. In order to improve the reproducibility between different laboratories, ISO 10140-1 has specified a preferred ratio of 2:1 of the depths of the niches on the two sides of the testing panel [8].

Modeling approaches to predict the STL accounting for the niche effect have already been developed. Kim *et al.* confirmed that the niche effect plays an important role in computing the STL in a laboratory [9]. Therefore, a two-dimensional system was considered, analyzing the test panel as an infinite strip with a finite height. Next, Vinokur defined the niche effect as the difference in STL between a panel placed at the center and at the edge of the aperture [10]. His model indicated that the STL is only influenced by the dimensions of the aperture, not by the parameters of the panel. Finally, Dijckmans and Vermeer [7] calculated the STL for single and double panels by means of a wave based method, which required a full coupling between the room modes, the niche modes, the cavity modes and the bending wave modes of the plates. In this case, the source and receiver rooms need to be modeled in detail and the results are only valid for the specific room geometries considered.

This paper aims to develop a numerical approach that uses a coupling between the finite element (FE) and the boundary element method (BE) to derive the radiation stiffness of the two rooms, which is applied to the special case of a niche. The air volume inside the niche is modeled with the FE, while the coupling to the acoustic halfspace is treated using the BE. The direct field dynamic stiffness matrices computed with a FE-BE model are then coupled with the deterministic model of the partition panel, in order to obtain the diffuse STL that relates to the average performance across many different laboratories, not to one specific laboratory.

This paper is organized as follows. Section 2 presents a general framework to compute the diffuse STL in a room-wall-room setting. Section 3 describes how the acoustic halfspaces at both sides of the panel are computed using a FE-BE coupling, accounting for the depth of the niches. Then, this methodology is applied in section 4 to the case of a laminated glazing and validated by comparing to measurements results. Finally, section 5 gives a conclusion to this paper.

## 2. Sound insulation prediction framework

The diffuse sound transmission loss is evaluated using the Det-SEA room-wall-room framework [1]. In this framework, the wall is modeled deterministically, while the source and receiver rooms are assumed to carry diffuse sound fields. A full derivation of the formulation can be found in [1]; only the main relations required for the present work are summarized here.

The diffuse transmission coefficient $\tau_{12}$ is defined as the ratio between the sound power transmitted from the source room (room 1) to the receiver room (room 2) $P_{\text{in}}^{(1\to 2)}$, and the incident sound power on the wall in the source room $P_{\text{inc}}^{(1)}$:

$$\tau_{12} := \frac{P_{\text{in}}^{(1\to 2)}}{P_{\text{inc}}^{(1)}}. \tag{1}$$

The diffuse STL $R$ of the partition panel is then computed as:

$$R = -10 \log \tau_{12} \tag{2}$$

If the source room carries a diffuse sound field, the ensemble mean of the incident power relates to the total energy of the room [11]:

$$\hat{P}_{\text{inc}}^{(1)} = \frac{c_0 S}{4V_1} \hat{E}_1, \tag{3}$$

where a hat denotes the mean across the diffuse random field ensemble, $c_0$ the sound speed in air, $S$ the surface area of the considered wall, $V_1$ the volume of the source room and $\hat{E}_1$ the mean total sound energy in the source room.

In the Det-SEA formulation, the acoustic field in each room is decomposed into a deterministic direct field and a random reverberant field. The direct field represents waves radiated away from the vibrating wall, whereas the reverberant field represents reflected waves traveling back towards the wall. The equations of motion for a single room $j$ is expressed as:

$$\mathbf{D}^{(j)}\mathbf{u} = \left(\mathbf{D}_{\text{dir}}^{(j)} + \mathbf{D}_{\text{rev}}^{(j)}\right)\mathbf{u} = \mathbf{f}^{(j)} \qquad j = 1, 2 \tag{4}$$

with $\mathbf{D}^{(j)}$ the acoustic dynamic stiffness matrix of the room, relating the displacements of the plate $\mathbf{u}$ and the forces $\mathbf{f}^{(j)}$ at the interface between the plate and the room. $\mathbf{D}^{(j)}$ has been decomposed into a deterministic direct field dynamic stiffness matrix $\mathbf{D}_{\text{dir}}^{(j)}$ and a random reverberant field dynamic stiffness matrix $\mathbf{D}_{\text{rev}}^{(j)}$.

The equations of motion of the wall-room-system are then:

$$\left(\mathbf{D}_{\text{tot}} + \mathbf{D}_{\text{rev}}^{(1)} + \mathbf{D}_{\text{rev}}^{(2)}\right)\mathbf{u} = \mathbf{f} \tag{5}$$

with

$$\mathbf{D}_{\text{tot}} = \mathbf{D}_{\text{d}} + \mathbf{D}_{\text{dir}}^{(1)} + \mathbf{D}_{\text{dir}}^{(2)}, \tag{6}$$

where $\mathbf{D}_{\text{d}}$ denotes the structural dynamic stiffness matrix of the plate. Since the ensemble mean of the reverberant dynamic stiffness matrices is zero, they are neglected in a first-order approximation. By applying the diffuse field reciprocity relationship [2], the mean sound power flow from the source room to the receiver room is:

$$\hat{P}_{\text{in}}^{(1\to 2)} = \frac{2\hat{E}_1}{\pi n_1}\text{Tr}\left(\text{Im}\left(\mathbf{D}_{\text{dir}}^{(1)}\right)\mathbf{D}_{\text{tot}}^{-\text{H}}\text{Im}\left(\mathbf{D}_{\text{dir}}^{(2)}\right)\mathbf{D}_{\text{tot}}^{-1}\right) \tag{7}$$

with $n_1$ the modal density in the source room [11]:

$$n_1 = \frac{\omega^2 V_1}{2\pi^2 c_0^3} \tag{8}$$

Combining the previous equations results in the final expression for the diffuse sound transmission coefficient:

$$\hat{\tau}_{12} = \frac{16\pi c_0^2}{S\omega^2}\text{Tr}\left(\text{Im}\left(\mathbf{D}_{\text{dir}}^{(1)}\right)\mathbf{D}_{\text{tot}}^{-\text{H}}\text{Im}\left(\mathbf{D}_{\text{dir}}^{(2)}\right)\mathbf{D}_{\text{tot}}^{-1}\right). \tag{9}$$

The evaluation of the ensemble average diffuse field transmission coefficient requires only the dynamic stiffness matrix of the wall and of the acoustic domains on both sides. For flat baffled panels, the direct field matrices can be obtained from a Rayleigh integral formulation, for instance using a wavelet discretization of the baffled interface [3]. However, this approach is restricted to flat radiating surfaces. In the following section, a FE-BE procedure is introduced to compute the direct field radiation stiffness of panels mounted in a niche.

## 3. Direct field radiation stiffness of a niche

This section describes the derivation of the direct field dynamic stiffness matrix $\mathbf{D}_{\text{dir}}$ for a panel mounted in a niche. In contrast to a flat baffled panel, the acoustic radiation is affected by the finite air volume inside the niche and by the position of the panel within the laboratory opening. As a result, the direct field radiation stiffness generally differs on both sides of the panel.

### 3.1. Niche geometry and interface partitioning

Fig. 2 schematically present a partition panel mounted in a laboratory opening, creating two niches at both sides. The air volumes inside the niches are modeled with FE and are bounded by the vibrating partition panel on one side and by the opening to the exterior acoustic halfspace on the other side, modeled with BE. The thick solid lines represent the rigid walls of the laboratory, on which a zero normal acoustic velocity is imposed.

The acoustic pressure degrees of freedom (DOFs) in the niche are partitioned into three sets. The DOFs at the opening towards the acoustic halfspace are denoted by $\mathbf{p}_{\text{t}}$. The DOFs located at the vibrating panel interface are denoted by $\mathbf{p}_{\text{b}}$. All remaining internal acoustic DOFs are denoted by $\mathbf{p}_{\text{i}}$.

The aim of the formulation is to obtain the direct field dynamic stiffness matrix at the physical interface of the partition panel, i.e. at the degrees of freedom associated with $\mathbf{p}_{\text{b}}$. This matrix relates the normal displacements of the panel to the acoustic forces exerted by the niche air volume on the panel.

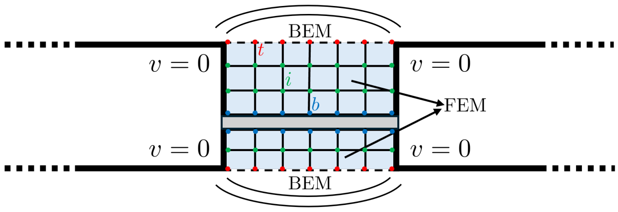


**Figure 2:** FE-BE representation of a niche geometry.

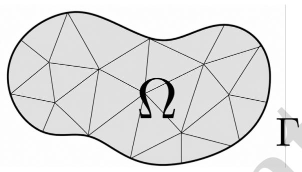


**Figure 3:** Schematic visualization of a FE domain.

### 3.2. FE model of the niche volume

The acoustic pressure field inside the niche is described using a pressure-based finite element formulation of the Helmholtz equation. For a general air volume $\Omega$, as illustrated in Fig. 3, the frequency-domain system of equations is expressed as [12]:

$$\mathbf{D}_{\text{a}}\mathbf{p} = \mathbf{f}_{\text{a}}, \tag{10}$$

where $\mathbf{p}$ collects the nodal acoustic pressures, $\mathbf{f}_{\text{a}}$ is the acoustic load vector associated with prescribed normal velocities on the boundary, and $\mathbf{D}_{\text{a}}$ is the acoustic dynamic stiffness matrix. For a lossless acoustic medium, this matrix is given by:

$$\mathbf{D}_{\text{a}} = -\omega^2\mathbf{M}_{\text{a}} + \mathbf{K}_{\text{a}}, \tag{11}$$

where $\mathbf{M}_{\text{a}}$ and $\mathbf{K}_{\text{a}}$ are the acoustic mass and stiffness matrices, respectively. For notational clarity, the subscript a is omitted in the following FE expressions. The global matrices are assembled from their element contributions. For an acoustic finite element with volume $\Omega_e$, the element mass matrix is given by:

$$\mathbf{M}_{\text{e}} = \int_{\Omega_{\text{e}}} \frac{1}{\rho_0 c_0^2}\mathbf{N}_{\text{e}}^{\text{T}}\mathbf{N}_{\text{e}}\,\text{d}V, \tag{12}$$

where $\mathbf{N}_{\text{e}}$ contains the acoustic shape functions, and $\rho_0$ is the density of air. The element stiffness matrix is obtained as:

$$\mathbf{K}_{\text{e}} = \int_{\Omega_{\text{e}}} \frac{1}{\rho_0}(\nabla\mathbf{N}_{\text{e}})^{\text{T}}\nabla\mathbf{N}_{\text{e}}\,\text{d}V. \tag{13}$$

A prescribed normal acoustic velocity on an arbitrary boundary $\Gamma$ introduces an acoustic boundary load. For an element boundary $\Gamma_{\text{e}}$, the corresponding load contribution is expressed as:

$$\mathbf{f}_{\text{e}} = \text{i}\omega\int_{\Gamma\text{e}} \mathbf{N}_{\text{e}}^{\text{T}}\mathbf{v}_n\,\text{d}S, \tag{14}$$

where $\mathbf{v}_n$ is the normal acoustic velocity on the boundary. After discretizing the boundary velocity field, the assembled boundary load can be expressed in matrix form as:

$$\mathbf{f} = \mathbf{T}_\Gamma \mathrm{i}\omega \mathbf{v}\Gamma, \tag{15}$$

where $\mathbf{T}_\Gamma$ maps the nodal normal velocities on the boundary $\Gamma$ to the acoustic FE load vector.

Applying this formulation to the niche geometry, using the introduced partitioning of the acoustic DOFs, gives:

$$\begin{bmatrix} \mathbf{D}_{\mathrm{tt}} & \mathbf{D}_{\mathrm{ti}} & \mathbf{D}_{\mathrm{tb}} \\ \mathbf{D}_{\mathrm{it}} & \mathbf{D}_{\mathrm{ii}} & \mathbf{D}_{\mathrm{ib}} \\ \mathbf{D}_{\mathrm{bt}} & \mathbf{D}_{\mathrm{bi}} & \mathbf{D}_{\mathrm{bb}} \end{bmatrix} \begin{bmatrix} \mathbf{p}_{\mathrm{t}} \\ \mathbf{p}_{\mathrm{i}} \\ \mathbf{p}_{\mathrm{b}} \end{bmatrix} = \begin{bmatrix} \mathbf{T}_{\mathrm{t}} \mathrm{i}\omega \mathbf{v}_{\mathrm{t}} \\ \mathbf{0} \\ \mathbf{T}_{\mathrm{b}} \mathrm{i}\omega \mathbf{v}_{\mathrm{b}} \end{bmatrix}. \tag{16}$$

Here, $\mathbf{v}_{\mathrm{t}}$ denotes the normal acoustic velocity at the acoustic halfspace, and $\mathbf{v}_{\mathrm{b}}$ denotes the normal velocity imposed by the vibrating partition panel.

### 3.3. BE radiation condition at the niche opening

The FE model introduced in the previous section describes the acoustic field inside the niche. To account for radiation from the niche opening into the adjacent room, the opening is coupled to an acoustic halfspace using a BE formulation. This provides a radiation condition at the interface degrees of freedom (t), without explicitly modeling the full source or receiver room geometry.

The boundary element method is based on a boundary integral representation of the Helmholtz equation and is particularly suited for exterior acoustic radiation problems [12]. For a boundary $\Gamma$, the pressure field at a receiver point $\mathbf{x}'$ can be expressed in terms of the acoustic pressure $\mathbf{p}$ and its normal derivative $\mathbf{q} = \partial\mathbf{p}/\partial\mathbf{n}$ at source points $\mathbf{x}$ on the boundary. Using the Green's function $\mathrm{G}(\mathbf{x}', \mathbf{x})$, the boundary integral equation reads [13]:

$$\mathbf{p}(\mathbf{x}') = \int_\Gamma \left( \mathbf{p}(\mathbf{x}) \frac{\partial \mathrm{G}(\mathbf{x}', \mathbf{x})}{\partial \mathbf{n}_{\mathbf{x}}} - \mathrm{G}(\mathbf{x}', \mathbf{x}) \mathbf{q}(\mathbf{x}) \right) \mathrm{d}S. \tag{17}$$

In the present case, a halfspace Green's function is used, such that the rigid baffle surrounding the niche opening is accounted for by the image source method [13].

The Green's function $\mathrm{G}(\mathbf{x}', \mathbf{x})$ and its normal derivative become singular when the receiver point $\mathbf{x}'$ approaches the source point $\mathbf{x}$ on the boundary. To treat this singular behavior, the integral equation is regularized by subtracting the corresponding static Green's function contribution [12]. This yields:

$$\mathbf{p}(\mathbf{x}') = \int_\Gamma \left( \mathbf{p}(\mathbf{x}) \frac{\partial \mathrm{G}(\mathbf{x}', \mathbf{x})}{\partial \mathbf{n}_{\mathbf{x}}} - \frac{\partial \mathrm{G}_0(\mathbf{x}', \mathbf{x})}{\partial \mathbf{n}_{\mathbf{x}}} \hat{p}(\mathbf{x}') \right) \mathrm{d}S - \int_\Gamma \mathrm{G}(\mathbf{x}', \mathbf{x}) \mathbf{q}(\mathbf{x}) \, \mathrm{d}S \tag{18}$$

where $\mathrm{G}_0$ denotes the static Green's function. This regularized form is used for the numerical boundary element discretization.

After spatial discretization of the boundary pressure and normal pressure gradient, Eq. (18) leads to the algebraic BE system

$$(\mathbf{Q} + \mathbf{I})\, \mathbf{p}_{\mathrm{t}} = \mathbf{P} \mathbf{q}_{\mathrm{t}}, \tag{19}$$

where $\mathbf{P}$ and $\mathbf{Q}$ are the boundary element system matrices at the niche opening.

Since the coupling interface between the niche and the acoustic halfspace is flat and lies in the rigid baffle plane, the contribution associated with the normal derivative of the halfspace Green's function vanishes. Consequently, $\mathbf{Q} = \mathbf{0}$, and Eq. (19) reduces to:

$$\mathbf{p}_{\mathrm{t}} = \mathbf{P} \mathbf{q}_{\mathrm{t}}. \tag{20}$$

The normal pressure gradient is related to the normal acoustic velocity by the linearized momentum equation, which gives combined with Eq. (20):

$$\mathbf{v}_t = -\frac{1}{\mathrm{i}\rho_0 \omega} \mathbf{q}_{\mathrm{t}} = -\frac{1}{\mathrm{i}\rho_0 \omega} \mathbf{P}^{-1} \mathbf{p}_{\mathrm{t}}. \tag{21}$$

Equation (21) expresses the radiation condition of the exterior halfspace as a relation between the pressure and normal velocity at the niche opening. Substituting this relation into the finite element system of Eq. (16) eliminates $\mathbf{v}_{\mathrm{t}}$ and yields:

$$\begin{bmatrix} \mathbf{D}^\star_{\mathrm{tt}} & \mathbf{D}_{\mathrm{ti}} & \mathbf{D}_{\mathrm{tb}} \\ \mathbf{D}_{\mathrm{it}} & \mathbf{D}_{\mathrm{ii}} & \mathbf{D}_{\mathrm{ib}} \\ \mathbf{D}_{\mathrm{bt}} & \mathbf{D}_{\mathrm{bi}} & \mathbf{D}_{\mathrm{bb}} \end{bmatrix} \begin{bmatrix} \mathbf{p}_{\mathrm{t}} \\ \mathbf{p}_{\mathrm{i}} \\ \mathbf{p}_{\mathrm{b}} \end{bmatrix} = \begin{bmatrix} \mathbf{0} \\ \mathbf{0} \\ \mathbf{T}_{\mathrm{b}} \mathrm{i}\omega \mathbf{v}_{\mathrm{b}} \end{bmatrix} \tag{22}$$

with $\mathbf{D}^\star_{\mathrm{tt}} = \mathbf{D}_{\mathrm{tt}} + \mathbf{T}_{\mathrm{t}} \mathbf{P}^{-1}/\rho_0$. Hence, the BE radiation condition is incorporated in the FE model by adding the derived radiation contribution to the interface equation at the niche opening.

### 3.4. Derivation of the direct field dynamic stiffness matrix

The direct field dynamic stiffness matrix $\mathbf{D}_{\mathrm{dir}}$ is defined as the matrix relating the displacements of the partition panel, $\mathbf{u}_{\mathrm{b}}$, to the acoustic forces acting on the panel, $\mathbf{f}_{\mathrm{b}}$:

$$\mathbf{D}_{\mathrm{dir}} \mathbf{u}_{\mathrm{b}} = \mathbf{f}_{\mathrm{b}}. \tag{23}$$

Starting from the coupled FE-BE system in Eq. (22), the internal acoustic degrees of freedom, denoted by the index i, are first eliminated. This condensation step is computationally beneficial, since the internal acoustic degrees of freedom typically represent the largest part of the finite element model. The reduced system, containing only the degrees of freedom at the niche opening and at the panel interface, is expressed as:

$$\begin{bmatrix} \mathbf{D}_{\mathrm{tt,eq}} & \mathbf{D}_{\mathrm{tb,eq}} \\ \mathbf{D}_{\mathrm{bt,eq}} & \mathbf{D}_{\mathrm{bb,eq}} \end{bmatrix} \begin{bmatrix} \mathbf{p}_{\mathrm{t}} \\ \mathbf{p}_{\mathrm{b}} \end{bmatrix} = \begin{bmatrix} \mathbf{0} \\ \mathbf{T}_{\mathrm{b}} \mathrm{i}\omega \mathbf{v}_{\mathrm{b}} \end{bmatrix} \tag{24}$$

with

$$\mathbf{D}_{\mathrm{tt,eq}} = \mathbf{D}^*_{\mathrm{tt}} - \mathbf{D}_{\mathrm{ti}}\mathbf{D}_{\mathrm{ii}}^{-1}\mathbf{D}_{\mathrm{it}} \tag{25}$$

$$\mathbf{D}_{\mathrm{tb,eq}} = \mathbf{D}_{\mathrm{tb}} - \mathbf{D}_{\mathrm{ti}}\mathbf{D}_{\mathrm{ii}}^{-1}\mathbf{D}_{\mathrm{ib}} \tag{26}$$

$$\mathbf{D}_{\mathrm{bb,eq}} = \mathbf{D}_{\mathrm{bb}} - \mathbf{D}_{\mathrm{bi}}\mathbf{D}_{\mathrm{ii}}^{-1}\mathbf{D}_{\mathrm{ib}} \tag{27}$$

$$\mathbf{D}_{\mathrm{bt,eq}} = \mathbf{D}_{\mathrm{bt}} - \mathbf{D}_{\mathrm{bi}}\mathbf{D}_{\mathrm{ii}}^{-1}\mathbf{D}_{\mathrm{it}}. \tag{28}$$

This condensed system of equations can then be solved for the degrees of freedom of the plate only:

$$\mathbf{D}_{\mathrm{b}}\mathbf{p}_{\mathrm{b}} = \mathbf{T}_{\mathrm{b}}\mathrm{i}\omega\mathbf{v}_{\mathrm{b}} \tag{29}$$

with

$$\mathbf{D}_{\mathrm{b}} = \mathbf{D}_{\mathrm{bb,eq}} - \mathbf{D}_{\mathrm{bt,eq}}\mathbf{D}_{\mathrm{tt,eq}}^{-1}\mathbf{D}_{\mathrm{tb,eq}}. \tag{30}$$

Using the relation between the normal velocity and displacement of the panel $\mathbf{v}_{\mathrm{b}} = \mathrm{i}\omega\mathbf{u}_{\mathrm{b}}$, the pressure at the panel interface follows from (29) as:

$$\mathbf{p}_{\mathrm{b}} = \mathbf{D}_{\mathrm{b}}^{-1}\mathbf{T}_{\mathrm{b}}\mathrm{i}\omega(\mathrm{i}\omega\mathbf{u}_{\mathrm{b}}). \tag{31}$$

The acoustic pressure at the panel interface is finally converted into equivalent forces acting on the partition panel, by equating $\mathbf{f}_{\mathrm{b}} = \mathbf{T}_{\mathrm{b}}\mathbf{p}_{\mathrm{b}}$. The direct field dynamic stiffness matrix of the niche is then obtained as:

$$\mathbf{D}_{\mathrm{dir}} = -\mathbf{T}_{\mathrm{b}}\mathbf{D}_{\mathrm{b}}^{-1}\mathbf{T}_{\mathrm{b}}\omega^2. \tag{32}$$

### 3.5. Modal projection and implementation in the diffuse STL model

The diffuse STL framework described in section 2 requires the deterministic structural dynamic stiffness matrix of the partition panel, $\mathbf{D}_{\mathrm{d}}$, and the direct field dynamic stiffness matrices, $\mathbf{D}_{\mathrm{dir}}^{(j)}$, on both sides of the panel. The latter are obtained from the FE-BE procedure described in the previous subsections. In the present implementation, the structural response of the partition panel is expressed in modal coordinates. This reduces the computational effort and allows the acoustic radiation stiffness matrices to be projected onto the same reduced basis.

In the modal basis, the structural dynamic stiffness matrix reads

$$\mathbf{D}_{\mathrm{d,mod}} = -\omega^2\mathbf{M}_{\mathrm{mod}} + \mathbf{K}_{\mathrm{mod}}, \tag{33}$$

where $\mathbf{M}_{\mathrm{mod}}$ is the modal mass matrix and $\mathbf{K}_{\mathrm{mod}}$ is the modal stiffness matrix.

The direct field dynamic stiffness matrices $\mathbf{D}_{\mathrm{dir}}^{(j)}$ are also projected onto the structural modal basis $\Phi$ as:

$$\mathbf{D}_{\mathrm{dir,mod}}^{(j)} = \mathbf{\Phi}^{\mathrm{T}}\mathbf{D}_{\mathrm{dir}}^{(j)}\mathbf{\Phi}, \qquad j = 1, 2. \tag{34}$$

## 4. Numerical application to a laminated glazing

The proposed methodology is applied to predict the sound transmission loss of a laminated glazing installed in a laboratory transmission opening. The numerical results are compared with experimental data obtained by Cops *et al.* in the transmission chambers of the Laboratory of Acoustics at KU Leuven [4]. The laminated glass panel has in-plane dimensions of $1.60 \times 1.30$ m$^2$ and consists of two 4 mm glass layers separated by a 0.76 mm butyl interlayer.

**Table 1:** Material properties of the equivalent single-layered representation of the laminated glazing.

| $\rho$ [kg/m$^3$] | $E$ [GPa] | $\eta$ [-] | $\nu$ [-] |
|---|---|---|---|
| 2500 | 52 | 0.10 | 0.24 |

The test panel is considered at two different positions inside the niche aperture in order to investigate the influence of the panel position on the measured and predicted STL. In the first configuration, the panel is placed close to one side of the opening, resulting in nominal niche depths of 0.00 m and 0.70 m. This position is further referred to as the edge niche. In the second configuration, the panel is placed nearly centrally in the opening, resulting in niche depths of 0.30 m and 0.40 m. This position is further referred to as the center niche.

For each configuration, the finite element model of the niche volume is constructed from the corresponding niche geometry and coupled to the boundary element model of the acoustic halfspace at the niche opening. The resulting FE-BE model is used to compute the direct field dynamic stiffness matrices on both sides of the glazing. For the edge niche configuration, effective niche depths of 0.05 m and 0.65 m are used in the numerical model to account for the frame against which the panel is mounted, following the approach suggested by Dijckmans *et al.* [7].

To compute the structural dynamic stiffness matrix $\mathbf{D}_{\mathrm{d}}$, the laminated glazing is represented as an equivalent single-layer panel with frequency-independent material properties. The equivalent material properties used in the model are listed in Table 1 [7]. The glazing is modeled as a thin, linear elastic, isotropic, simply supported rectangular plate, such that both $\mathbf{D}_{\mathrm{d}}$ and $\Phi$ can be obtained analytically [14].

Fig. 4 compares the predicted sound transmission loss with the measured values for both panel positions. Overall, a good agreement is obtained between the FE-BE predictions and the experimental results. The model captures the difference in STL between the edge and center niche configurations below the critical frequency, which confirms that the proposed direct field radiation stiffness formulation is able to account for the influence of the niche geometry. Above the critical frequency, the influence of the panel position becomes negligible in both the measurements and the numerical predictions.

Around the critical frequency, some deviations between the numerical and experimental results are observed. These discrepancies can be attributed, at least partly, to the simplified equivalent single-layer representation of the laminated glazing and to uncertainties in its actual damping. Nevertheless, the comparison demonstrates that the proposed FE-BE procedure correctly captures the main influence of the panel position inside the laboratory niche.

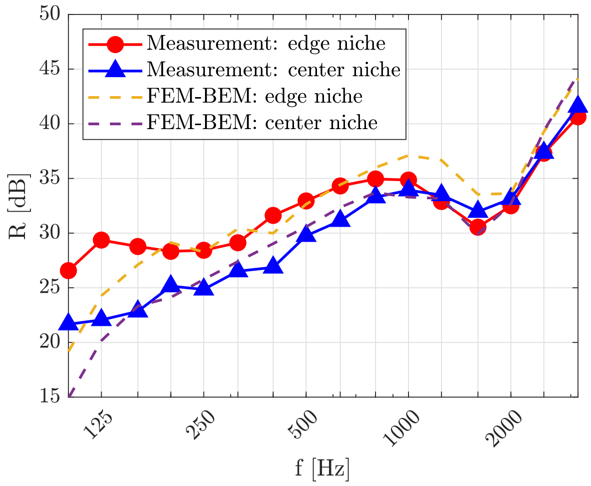


**Figure 4:** Diffuse STL for the edge and center niche: measurement results [4] and FE-BE predictions.

## 5. Conclusion

The aim of this paper was to develop a numerical method to compute the diffuse sound transmission loss of partition panels, while taking into account the effect of a niche, by using a FE-BE approach.

The proposed approach builds on an existing hybrid deterministic-statistical energy analysis room-wall-room framework, in which the partition panel is modeled deterministically and the source and receiver rooms are represented by diffuse sound fields. In this framework, the diffuse sound transmission coefficient can be expressed in terms of the deterministic dynamic stiffness matrix of the panel and the direct field dynamic stiffness matrices of the acoustic domains on both sides of the panel.

The main contribution of this work is the derivation of these direct field dynamic stiffness matrices for non-flat geometries, and for the special case of a partition panel mounted in a niche. The acoustic volume inside the niche is modeled using FE, while the radiation from the niche opening into the adjacent acoustic halfspace is represented using a BE formulation.

The methodology was applied to a laminated glazing installed at different positions in a laboratory transmission opening. The predicted STL values were compared with experimental results, showing that the FE-BE approach captures the influence of the panel position in the niche. Good agreement was obtained for the considered configurations, although deviations were observed around the critical frequency. These deviations are likely related to the simplified equivalent single-layer representation of the laminated glazing and to uncertainties in the actual damping and mounting conditions.

Overall, the proposed methodology provides a good way to include laboratory niche effects in diffuse sound insulation predictions, without explicitly modeling the full source and receiver rooms.

## References


[1] E. Reynders and C. Van hoorickx, "Uncertainty quantification of diffuse sound insulation values," *Journal of Sound and Vibration*, vol. 544, no. 117404, pp. 1–15, 2023.

[2] P. Shorter and R. Langley, "On the reciprocity relationship between direct field radiation and diffuse reverberant loading," *J. Acoust. Soc. Am.*, vol. 117, no. 1, pp. 85–95, 2005.

[3] R. Langley, "Numerical evaluation of the acoustic radiation from planar structures with general baffle conditions using wavelets," *J. Acoust. Soc. Am.*, vol. 121, no. 2, pp. 766–777, 2007.

[4] A. Cops, M. Minten, and H. Myncke, "Influence of the design of transmission rooms on the sound transmission loss of glass - Intensity versus conventional method," *Noise Control Engineering Journal*, vol. 28, no. 3, pp. 121–129, 1987.

[5] A. Osipov, P. Mees, and G. Vermeir, "Low-frequency airborne sound transmission through single partitions in buildings," *Applied Acoustics*, vol. 52, no. 3–4, pp. 273–288, 1997.

[6] T. Kihlman and A. Nilsson, "The effect of some laboratory design and mounting conditions on reduction index measurements," *Journal of Sound and Vibration*, vol. 24, no. 3, pp. 349–364, 1972.

[7] A. Dijckmans and G. Vermeir, "A wave based model to predict the niche effect on sound transmission loss of single and double walls," *Acta Acustica united with Acustica*, vol. 98, pp. 111–119, 2012.

[8] *ISO 10140-1: Acoustics – Laboratory measurement of sound insulation of building elements – Part 1: Application rules for specific products*, International Organization for Standardization, 2021.

[9] B.-K. Kim, H.-J. Kang, J.-S. Kim, H.-S. Kim, and S.-R. Kim, "Tunneling effect in sound transmission loss determination: Theoretical approach," *J. Acoust. Soc. Am. 115*, (2004) 2100-2109.

[10] R. Vinokur, "Mechanism and calculation of the niche effect in airborne sound transmission," *J. Acoust. Soc. Am.*, vol. 119, pp. 2211–2219, 2006.

[11] R. Lyon and R. DeJong, *Theory and application of statistical energy analysis*, second. Newton, MA: Butterworth-Heinemann, 1995.

[12] N. Atalla and F. Sgard, *Finite element and boundary element methods in structural acoustics and vibration*. Boca Raton, FL: CRC Press, 2015.

[13] M. Bonnet, *Boundary integral equation methods for solids and fluids*. John Wiley and Sons, Chichester, United Kingdom, 1995.

[14] J. Rindel, *Sound insulation in buildings*. Boca Raton, FL: CRC Press, 2018.